

Pump-Probe Delay Controlled by Laser-dressed Ionization with Isolated Attosecond Pulses

Martin Luttmann^{1*}, *David Bresteau*¹, and *Thierry Ruchon*^{1**}

¹Université Paris-Saclay, CEA, CNRS, LIDYL, 91191 Gif-sur-Yvette, France

Abstract. In a recent work [1], we demonstrated how laser-dressed ionization can be harnessed to control with attosecond accuracy the time delay between an extreme-ultraviolet (XUV) attosecond pulse train and an infrared (IR) femtosecond pulse. In this case, the comb-like photoelectron spectrum obtained by ionizing a gas target with the two superimposed beams exhibits peaks oscillating with the delay. Two of them can be found to oscillate in phase quadrature, allowing an optimal measurement and stabilization of the delay over a large range. Here we expand this technique to isolated attosecond pulses, by taking advantage of the delay-modulation of attosecond streaking traces. Although the photoelectron spectrum contains no peaks in that case, it is possible to reconstruct the pump-probe delay by simply monitoring the mean energy of the spectrum and the amplitude at this energy. In general, we find that active delay stabilization based on laser-dressed ionization is possible as long as the XUV pulses are chirped.

1 Introduction

Attosecond pump-probe experiments require to control, with sub-femtosecond precision, the delay between two ultrashort light pulses. One of them is usually intense and in the Vis-infrared (IR) spectral range, while the second is weak and in the extreme-ultraviolet (XUV) spectral range. In order to perform experiments asking for high statistics, such a stability should be maintained over hours, while scanning the delay. This can only be achieved through active stabilization schemes, usually relying on the live measurement of interferences from an additional continuous laser beam co-propagating in the interferometer [2]. Such techniques have drawbacks: they require many additional optics, and most importantly do not provide an *in situ* control of the delay. Indeed, what is actually stabilized is the optical path difference accumulated by the continuous laser, which may differ from the XUV/IR optical path difference. In a previous work [1], we introduce a new technique, named LIZARD (Laser-dressed IoniZation for the Adjustment of the pump-pRoBe Delay), which does not require any such additional laser beam and allows an *in-situ* delay control. We implemented LIZARD on an attosecond beamline delivering attosecond pulses trains (APT), reaching an excellent delay stability. The goal of this paper is to show how LIZARD can also be applied to the stabilization of interferometers that use isolated attosecond pulses (IAP, i.e. attosecond pulses that do not come in trains). Such light sources are now routinely used in experiments [3] and would draw great benefits from the stability provided by LIZARD. We first recall the basic principle of the technique, then expand it to IAP.

2 Principle of LIZARD

When performing scans of the delay, one has to be able to continuously lock the pump-probe phase at arbitrary set-points, with a uniform stability. A solution consists in using two sinusoidal signals oscillating with the delay, which are in phase quadrature [5]. The principle of LIZARD is to extract those signals from two-photon photoelectron spectra obtained by photoionizing a gas target in an electronic spectrometer, with the superimposed XUV and IR beams. In the case of laser-dressed ionization by APT, the spectra typically show a series of peaks corresponding to the XUV harmonic energies; and sidebands in-between two harmonic peaks, oscillating with the delay [4]. Interestingly, the natural frequency chirp of attosecond pulses trains obtained via high harmonic generation (better known as "atto-chirp") guarantees that, in most practical cases, two sidebands close to phase quadrature can be found, regardless of the gas chosen or the intensity of the driving laser. The signal of such sidebands are used in the active stabilization loop. Small delay fluctuations are measurable, since at least one of the signals has a significant derivative, for any given delay. The phase quadrature hence guarantees that LIZARD provides an optimal and uniform stability over the whole optical cycle. The sidebands signals amplitude and offset first have to be calibrated. To do so, a fast delay scan is performed (during which we consider that unintended delay fluctuations do not occur), and the sidebands modulation is fitted with sines.

This technique was successfully implemented on the FAB10 beamline at the ATTOLab facility (CEA Saclay) [1]. The signal of two sidebands, separated in energy by 12 eV, and in phase by 0.46π rad, was used to perform

*e-mail: martin.luttmann@cea.fr

**e-mail: thierry.ruchon@cea.fr

the active stabilization. Despite an interferometer length of several meters, a long term delay stability of 28 as RMS was achieved.

3 Expansion of the technique to isolated attosecond pulses

Isolated attosecond pulses can be generated through various schemes. HHG can be driven by few or single cycle IR pulse. The electric field of such pulses peaking only once, XUV light is emitted in a single electron recombination event, which results in IAP. Other techniques use polarization gating [6] or double-optical gating [7]. In all cases, the suppression of the $T_0/2$ periodicity of the emitted light (with T_0 the IR period) yields an XUV supercontinuum in the frequency domain. It is thus not possible to obtain delay-oscillating sidebands. A variant of LIZARD may still be implemented, that we refer to as LIZARD-IAP. It also relies on laser-dressed photo-ionization of a gas target by the XUV pulse (Fig. 1), but in the "attosecond streaking" [8] or FROG-CRAB [9] regime. It corresponds to an intensity of the dressing laser field of about 10^{13} W/cm² instead of about 10^{11} W/cm² in the previously used RABBITT regime.

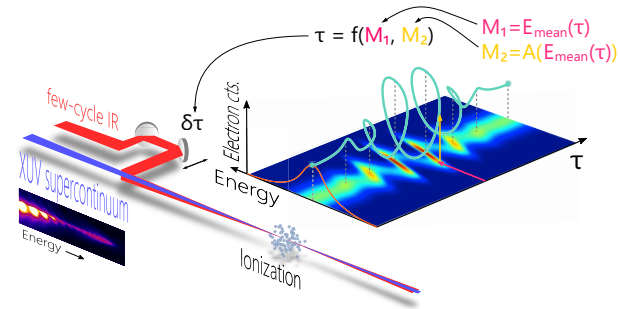


Figure 1. Principle of LIZARD-IAP. A feedback loop is performed in order to stabilize the XUV/IR delay τ , whose inputs are two quantities extracted from the streaked photoelectron spectrum: the mean energy ($M_1(\tau)$, vivid pink arrow) and the amplitude at this energy ($M_2(\tau)$, yellow arrow). If the XUV pulse is chirped, the correlation of these two quantities draws an ellipse (cyan curve). The delay τ can be reconstructed unambiguously, and any variation from the set-point value is compensated using two mirrors mounted on a piezo-electric stage. The streaking trace used in the figure is extracted from [10].

We consider an electron suddenly freed in a continuum state by absorption of an XUV photon, in the presence of a strong IR streaking field. The XUV field is denoted \mathbf{E}_{XUV} , the IR vector potential is \mathbf{A} , they are delayed in time by τ . The atom ionization energy is I_p . In the frame of first order perturbation theory, the probability amplitude for a photoelectron to have the momentum \mathbf{p} in the continuum, and the energy $W = \mathbf{p}^2/2$, writes [11]

$$a_{\mathbf{p}}(\tau) = -i \int_{-\infty}^{+\infty} dt e^{i\phi(t)} \mathbf{d}_{\mathbf{p}(t)} \cdot \mathbf{E}_{XUV}(t - \tau) e^{i(W+I_p)t}, \quad (1)$$

with

$$\phi(t) = - \int_t^{+\infty} dt' (\mathbf{p} \cdot \mathbf{A}(t') + A^2(t')/2). \quad (2)$$

$\mathbf{d}_{\mathbf{p}(t)}$ is the dipole transition matrix element from the ground state to the continuum state. $\phi(t)$ is the phase accumulated by the electron freed at time t , under the influence of an IR field. The effect of this streaking field is therefore to modulate the phase of the electron wave-packet (EWP), which in general results in distortion and shift of the photoelectron spectrum.

We propose here an intuitive explanation of the effect of the streaking field. In a semi-classical model, the atom is ionized at time t_i by the XUV field, an electron being ejected with an initial momentum \mathbf{p}_0 . Discarding effects of the atomic potential, the electron accelerates classically in the continuum under the influence of the streaking IR field. Since we have $\partial \mathbf{p} / \partial t = -\mathbf{E}_{IR} = \partial \mathbf{A} / \partial t$, the quantity $\mathbf{p}(t) - \mathbf{A}(t)$ is constant during this acceleration. Its final value equals the final momentum \mathbf{p}_f of the electron, as the IR field vanishes for long times. Therefore, the momentum of the electron is shifted by the IR potential at the time of ionization: $\mathbf{p}_f = \mathbf{p}_0 - \mathbf{A}(t_i)$, which means that the photoelectron average energy will oscillate with the XUV/IR delay (see Fig.2.a).

To get more insights on the effect of the EWP phase modulation, we consider the specific case of a sinusoidal IR field with a slowly varying envelope $\mathbf{E}_{IR}(t) = -\partial \mathbf{A} / \partial t = \mathbf{E}_0(t) \cos(\omega_0 t)$. While this approximation is clearly not valid for few-cycle pulses, it will still help deepening our general understanding. The phase modulation is given by [11]

$$\begin{aligned} \phi(t) &= \phi_1(t) + \phi_2(t) + \phi_3(t) \\ \text{with } \phi_1(t) &= - \int_t^{+\infty} dt U_p(t), \\ \phi_2(t) &= \frac{\sqrt{8WU_p(t)}}{\omega_0} \cos \theta \cos(\omega_0 t), \\ \phi_3(t) &= - \frac{U_p(t)}{2\omega_0} \sin(2\omega_0 t). \end{aligned} \quad (3)$$

In the above equations, U_p and θ are respectively the ponderomotive energy of the field and the angle between the momentum \mathbf{p} and the laser polarization direction. We restrain our analysis to $\theta = 0$ and $U_p \ll W$, hence ϕ_2 dominates over the two other terms.

We simulate photoelectron spectra of Ar gas ionized by a single attosecond pulse in the presence of a time-delayed low-frequency few-cycle IR field (Fig. 2). The duration of the gaussian XUV pulse is set at 300 as, the attochirp can be adjusted. We consider a gaussian, 4 fs, 800 nm central wavelength, 10^{13} W/cm² peak intensity dressing pulse with a null CEP. The temporal phase modulation of the EWP is calculated from Eq. 2. The energy vs delay trace is generated by computing the outer product of the two fields, and Fourier transform it along one dimension.

For a given delay τ between the two pulses, the photoelectron spectra in Fig. 2 are continuous, which is characteristic of ionization by IAP. The mean energy and peak amplitude vary with the delay, which can be understood by

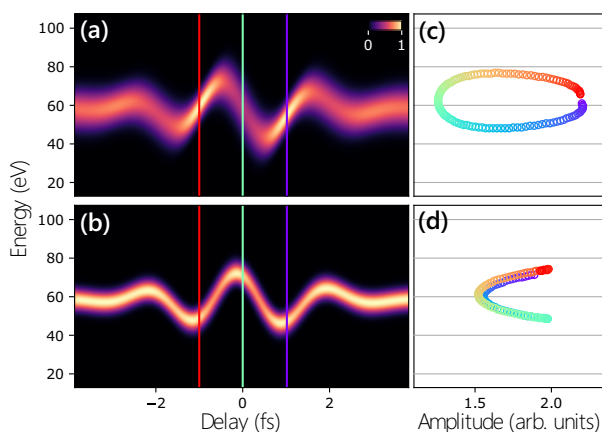


Figure 2. (a,b) Simulated attosecond streaking traces, with a $3 \times 10^2 \text{ fs}^{-2}$ atto-chirp (a), and with a null atto-chirp (b). (c,d) Corresponding correlation graphs between the mean energy (vertical axis) and the amplitude at this energy (horizontal axis), for delays varying between the red and blue vertical lines in (a,b). The delay is increasing from red to blue, and the horizontal axis of (c) and (d) have the same scale.

considering Eq. 3. When the attosecond pulse is synchronized with a zero of the IR field, the phase modulation is quasi-linear in the neighborhood of the pulse. This corresponds to a frequency shift of the whole spectrum (without distortion) towards high or low energies depending on whether the field amplitude is decreasing or increasing. In the case where the attosecond pulse is synchronized with a maximum of the IR field, the phase modulation is quadratic, and its effect adds up to the atto-chirp, yielding a spectral broadening and a decrease of the peak amplitude of the photoelectron spectrum. This is the case, for instance, along the green vertical line in Fig. 2.a. Conversely, when the attosecond pulse is synchronized with a minimum of the streaking field, the two effects partially compensate each other, yielding a narrower spectrum and a higher peak amplitude (red and purple lines in Fig. 2.a). Therefore, the photoelectron mean energy $E_{\text{mean}}(\tau)$ and the amplitude at this energy $A(E_{\text{mean}}(\tau))$ are in phase quadrature (Fig. 1), which provides an optimal stability. Such an asymmetry in the streaking trace is a signature of frequency chirp, and is key to LIZARD: the XUV frequency chirp allows to discriminate between a maximum and a minimum of the IR amplitude, hence to measure the pump-probe delay over the whole IR period. This conclusion applies both for LIZARD with APT and LIZARD-IAP.

We test these predictions with the simulated streaking traces. In Fig. 2.c, we display the mean energy of the spectrum vs the amplitude at this energy, as the delay is varied over one IR period. The correlation graph takes the form of an ellipsoid, i.e. the time delay is encoded azimuthally and can be reconstructed. When the attosecond pulse has no chirp (Fig. 2.c), the graph collapses, several points ending up at the same angle, preventing delay retrieval over the whole optical cycle. Just like regular LIZARD,

LIZARD-IAP needs a preliminary calibration of the ellipse, consisting in a fast delay scan.

We must highlight that LIZARD-IAP requires carrier-phase-envelope (CEP) stabilization, since changes of the CEP affect dramatically the streaking spectrum. Such stabilization loops are routinely used in beamlines delivering IAP along with single-cycle IR pulses. Conversely, if the interferometer is stabilized by another mean, monitoring the mean energy and peak amplitude of the photoelectron spectrum could be a way to access the CEP.

4 Conclusion

We have shown that the LIZARD technique, allowing active stabilization of the time delay between an attosecond and a femtosecond light pulse, can be applied to IAP. LIZARD requires two phase quadrature signals that are modulated with the delay; such signals can be extracted from the spectrum obtained by photo-ionizing a gas target with the two superimposed beams, in the FROG-CRAB regime. Provided that the IAP are chirped, the mean energy of the photoelectron spectrum and the amplitude at this energy vary with the delay and are $\pi/2$ out of phase.

The LIZARD-IAP technique is robust with respect to the experimental conditions. It is indeed applicable with any IR intensity (provided that it remains in the FROG-CRAB regime, i.e. about 10^{13} W/cm^2), any value of the atto-chirp (as long as it is significant), and regardless of the gas chosen.

The concepts developed here could be applied to the spectrograms obtained with free-electron-lasers (FEL). Such instruments are currently reaching attosecond durations, delivering sub-femtosecond XUV pulses. FEL, however, cannot provide sub-cycle synchronization between the XUV and IR field. It was shown in the case of multiple harmonics that an analysis of the correlation between the different sidebands fluctuations provides a measurement of the temporal jitter [12, 13]. We believe that a similar post-treatment can be made when the X-ray field consists of IAP. The correlation between the mean energy of the photoelectron spectrum and the peak amplitude would take the shape of an ellipse, allowing the retrieval of the pump-probe delay.

References

- [1] M. Luttmann *et al*, Phys. Rev. Applied **15**, 034036 (2021)
- [2] F. Böttcher *et al*, Applied Physics B **91**, 287–293 (2008)
- [3] M. Chini *et al*, Nature Photon **8**, 178-186 (2014)
- [4] V. Vényard *et al*, Phys. Rev. A **54**, 721 (1996)
- [5] V. V. Krishnamachari *et al*, Opt. Express **14**, 5210 (2006)
- [6] P. B. Corkum *et al*, Opt. Lett. **19**, 1870-1872 (1994)
- [7] H. Mashiko *et al*, Phys. Rev. Lett. **10**, 103906 (2008)
- [8] J. Itatani *et al*, Phys. Rev. Lett. **88**, 173903 (2002)
- [9] Y. Mairesse *et al*, Phys. Rev. A. **71**, 011401 (2005)

- [10] L. Cattaneo *et al*, Opt. Express **25**, 29060-29076 (2016)
- [11] F. Quéré *et al*, Journal of Modern Optics **52**, 339-360 (2005)
- [12] P.K. Maraju *et al*, Nature **578**, 386–391 (2020)
- [13] C. Krüger *et al*, Opt. Express **28**, 12862-12871 (2020)